Turkish Journal of Electrical Engineering and Computer Sciences

Volume 26 | Number 6 Article 14

1-1-2018

SAR image time-series analysis framework using morphological operators and global and local information-based linear discriminant analysis

UFUK SAKARYA

CANER DEMİRPOLAT

Turkish Journal of Electrical Engineering & Computer Sciences

http://journals.tubitak.gov.tr/elektrik/

Research Article

Turk J Elec Eng & Comp Sci
(2018) 26: 2958 – 2966

doi:10.3906/elk-1712-339

SAR image time-series analysis framework using morphological operators and global and local information-based linear discriminant analysis

Ufuk SAKARYA*, Caner DEMİRPOLAT
Space Technologies Research Institute (UZAY), Scientific and Technological Research Council of Turkey (TÜBİTAK), Ankara, Turkey

Received: 25.12.2017 • **Accepted/Published Online:** 13.08.2018 • **Final Version:** 29.11.2018

Abstract: Fusion of spectral, spatial, and temporal information is an effective method used in many satellite remote sensing applications. On the other hand, one drawback of this fusion is an increase in complexity. In this paper, we focus on developing a fast and well-performed classification method for agricultural crops using time-series SAR data. In order to achieve this, a novel two-stage approach is proposed. In the first stage, a high-dimensional feature space is obtained using time-series dual-pol SAR data and morphological operators. Spectral, spatial, and temporal information is combined into a single high-dimensional feature space. In the second stage, a dimension reduction technique is applied to the feature vector in order to decrease time complexity and increase classification accuracy by considering the global and local pattern information in the high-dimensional feature space. The contribution of the morphological profiles to the classification performance is significant; however the time complexity is increased drastically. The proposed method overcomes the time complexity stemming from high-dimensional feature space; it also improves the classification performance. The superiority of the proposed method to the comparative methods in agricultural crop classification is experimentally shown with the improvements in both classification and time performance using time-series TerraSAR-X images.

Key words: Remote sensing, SAR image time series, dimension reduction, morphological operators, crop classification

1. Introduction

Agricultural crop classification is usually an initial step in farming activities, food security, and precision agriculture. Remote sensing can provide a more practical way than conventional methods in agricultural practices and can be an effective tool in agricultural crop classification. Synthetic aperture radar (SAR) is not dependent on daylight, unlike optical sensors, and can capture information of plant structure; thus, it can become a powerful tool in crop monitoring like optical sensors. Crop classifications with multitemporal, multipolarization SAR data are studied by many researchers [1–4]. Some studies focused on classification with high-dimensional feature space extracted by polarimetric multifrequency SAR data [5–7]. Demirkesen et al. [8] proposed the use of morphological opening and closing profiles for crop classification with multitemporal SAR images. Demirpolat and Teke [9] used a larger SAR dataset and derived a larger number of morphological profiles for crop classification, obtaining a high-dimensional feature space; however, no dimension reduction was considered in this work. It has been shown that dimension reduction improves the classification and time performance for high-dimensional SAR datasets [10].

*Correspondence: ufuk.sakarya@tubitak.gov.tr

The curse of dimensionality is the problem of increasing complexity to structure a high-dimensional space caused by the exponential increase in training data size needed [11]. Many dimension reduction methods have been proposed to solve this problem. Two of the most well-known techniques are principal component analysis (PCA) [11] and linear discriminant analysis (LDA) [11]. PCA is an unsupervised method; on the contrary, LDA is a supervised one. PCA aims to find a projection by using eigenvectors of a scattering matrix of all data. LDA's objective is to find a projection to which members of the same classes are close and for which members of the different classes are far from each other [11]. LDA disregards the structure of local information and focuses on deriving global structure information [12]. A more comprehensive method for dimension reduction, which takes local similarity into account, has been proposed by the complete global-local LDA method (CGLDA) [12]. CGLDA models the local structure information by integrating two additional scattering matrices into the objective function. CGLDA has been applied to remote sensing data acquired with various sensors. It was experimentally shown that CGLDA provided better classification accuracies for hyperspectral data [13]. Similar results were obtained for multitemporal dual polarized SAR data [14] and thermal infrared hyperspectral data [15].

This work can be considered as an effective combination of [8,9,14]. Morphological profiles were first used in [8] for agricultural crop classification with multitemporal SAR data. A larger SAR dataset was used in [9] and the optimal size of morphological profiles to be used in classification was found to be around 20 for the experimental setup that had produced a high-dimensional feature space. Neither [8] nor [9] used any dimension reduction approaches. Sakarya and Demirpolat [14] first suggested dimension reduction with the CGLDA method on a time-series SAR data vector formed by backscattering in different polarizations. The proposed method fuses the feature extraction by morphological profiles and dimension reduction methods and also incorporates original backscattering channels into classification, unlike [8] and [9], to provide considerable improvements in classification and time performance.

This paper is organized as follows: Section 2 describes morphological profiles as the feature extraction method and LDA and CGLDA as dimension reduction techniques. Section 3 presents the proposed method. Section 4 gives information about the dataset, ground truth, and experiments and presents the results and comments. Finally, conclusions are given in Section 5.

2. Background

2.1. Morphological profiles

Opening [16] by reconstruction $\gamma^s(I)$ of an image I can be computed as a consequent morphological erosion and dilation operations by a structuring element of size s. The duality condition applies for closing by reconstruction $\varphi^s(I)$; it can be defined as a dilation of the original image I with structuring element of size s followed by reconstruction by erosion operation. When opening by reconstruction is computed on the image with a structuring element of increasing size, a morphological opening profile is derived from an image when opening by reconstruction is applied consecutively with a structuring element of increasing size [16]:

$$\pi_\gamma(I) = \{\, \pi_{\gamma k} : \pi_{\gamma k} = \gamma^k(I),\, \forall k \in [0,\ldots,n] \,\} \tag{1}$$

Identically, a morphological closing profile is derived by applying closing by reconstruction [16]:

$$\pi_\varphi(I) = \left\{\, \pi_{\varphi k} : \pi_{\varphi k} = \varphi^k(I),\, \forall k \in [0,\ldots,n] \,\right\} \tag{2}$$

A morphological profile is simply the concatenation of closing and opening profiles of size n and the original image, which results in a stack of $2n+1$ images.

2.2. LDA and CGLDA

The within-class scattering matrix S_W and the between-class scattering matrix S_B are calculated using the samples and class information in a set, which are later used for solving the objective function of LDA given by:

$$W_{LDA} = \arg\max_{W} \left| \frac{W^T S_B W}{W^T S_W W} \right| \tag{3}$$

Here, W^T is the transpose of matrix W.

The CGLDA method includes two new scattering matrices, the total local pattern variation scatter matrix S_{TL} and the local within-class scatter matrix S_{LW}, in addition to S_W and S_B. The objective function of CGLDA is:

$$W_{CGLDA} = \arg\max_{W} \left| \frac{W^T \left[\alpha S_B + (1-\alpha) S_{TL}\right] W}{W^T \left[\varepsilon S_W + (1-\varepsilon) S_{LW}\right] W} \right| \tag{4}$$

Parameter ε sets the ratio of local similarity and global similarity, where parameter α determines the ratio of local discriminant information to global discriminant information. Both parameters have to be in the range from 0 to 1. More details about the dimension reduction process applied in this work can be found in [12].

3. The proposed method

In this paper, a novel two-stage classification method for SAR image time-series data is proposed. The architecture of the proposed method can be seen in Figure 1. In the first stage, high-dimensional vector space is obtained using not only SAR image time-series data but also morphological operators. In the second stage, high-dimensional vector space is reduced in order to both decrease time complexity and increase classification accuracy.

3.1. Obtaining high-dimensional feature space

First, by combining original backscattering information with morphological opening and closing profiles derived from multitemporal dual-pol TerraSAR-X images, a high-dimensional vector space is obtained. The detected products are delivered in multilook ground range detected (MGD) format. ESA's Sentinel Application Platform (SNAP) software is used for absolute radiometric calibration and terrain-correction [17]. All SAR backscattering images and ground truth are registered. Speckle noise is a granular salt-and-pepper-like noise, which degrades the quality and interpretability of the SAR images. A speckle-reducing anisotropic diffusion (SRAD) filter [18] is used for reducing speckle noise due to its ability to preserve the edges, considering that there are more than 20 individual parcels in the study area. Ten morphological opening images and 10 morphological closing images are obtained from each channel of the processed time-series SAR backscattering images to form the high-dimensional vector space. The shape of the structuring element is selected as a disk and the initial radius is selected as one pixel. The structuring element's radius is increased by one in calculation of each morphological opening or closing image. This feature space can be considered as the unity of spectral, spatial, and temporal information derived from time-series SAR backscattering images.

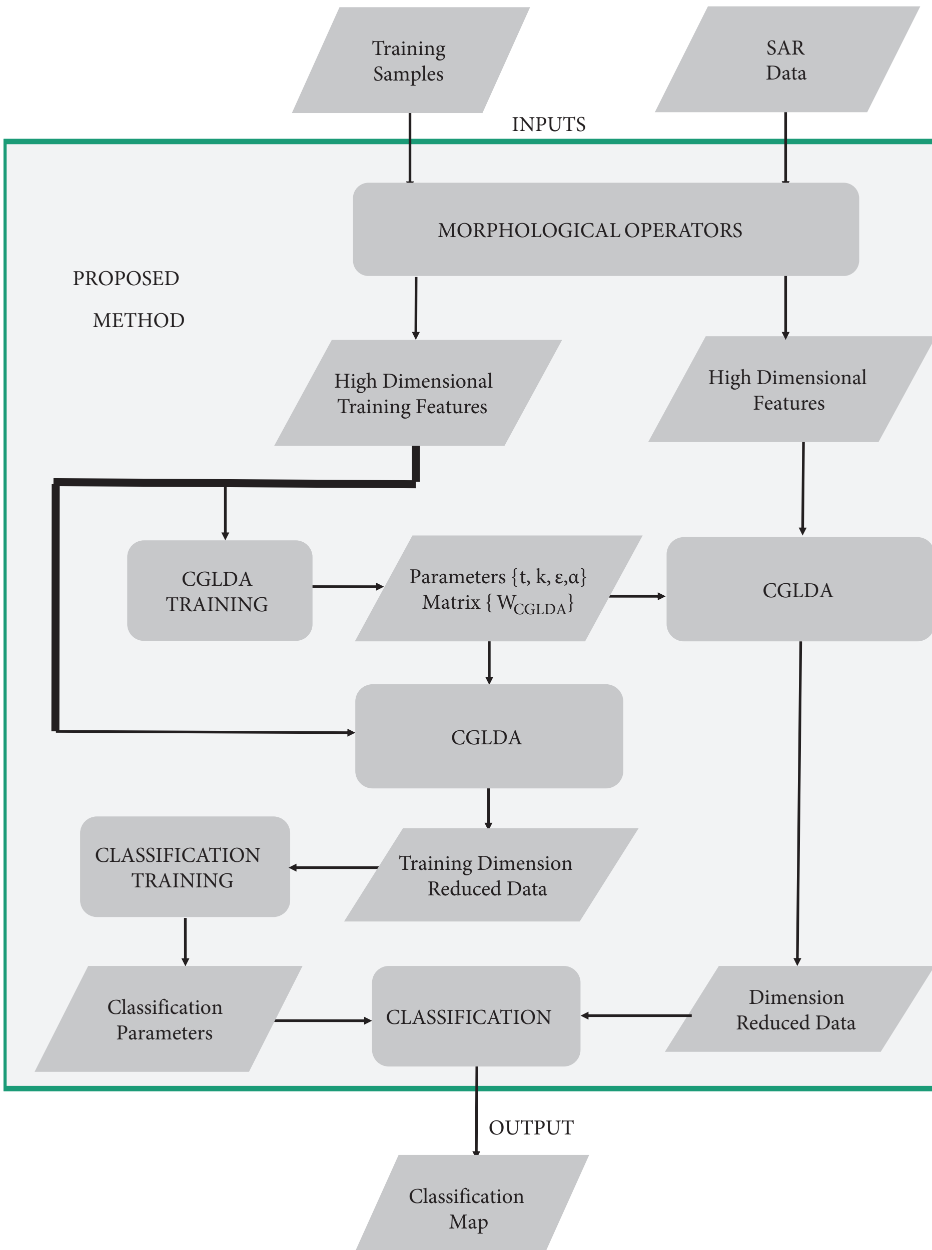

Figure 1. Architecture of the proposed method.

3.2. Dimension reduction

In the second stage, the high-dimensional vector space is reduced in order both to decrease complexity and increase classification accuracy. Global and local pattern information in high-dimensional space is utilized by dimension reduction for improving the performance. The CGLDA method is used for dimension reduction and classification is applied by using a dimensionally reduced vector space. In this study, the K-nearest neighbor (KNN) [11] technique is selected for classification due to its simplicity. KNN is a technique that memorizes all the instances of the training data and classifies new instances with regard to similarity measures such as

Euclidean, etc. Research for the best classifier is out of the scope of this paper since our research focuses on the right dataset, features, and dimension reduction methods.

4. Experiments and results

4.1. Description of dataset and ground truth

In this study, dual-polarized (HH + VV) TerraSAR-X images acquired on 10 May, 1 June, 23 June, 15 July, 6 August, 17 August, 28 August, and 19 September 2016 are used. Eight images with 2 polarization channels result in a feature space length of 16 for each pixel. TerraSAR-X images were acquired in SpotLight (SL) mode having range resolution of 3 m and azimuth resolution of 3.5 m. Incidence angles for all images are around 40 degrees.

Ground truth data were collected on 19 August 2016 via field measurements. There are 10 classes in the ground truth and the total number of samples (pixels) is 638,290. The classes are pistachio garden, wheat followed by corn, wheat followed by stubble, cotton, olive garden, pasture, pomegranate garden, wheat followed by cabbage, pepper, and greenwood. Wheat followed by corn, cotton, and pasture fields form the majority of the classes. Figure 2 shows the ground truth map of the study area. Color corresponds to the fields that are not used in the classification since no crops are grown in these fields. Numbers 1–10 correspond to aforementioned crop classes.

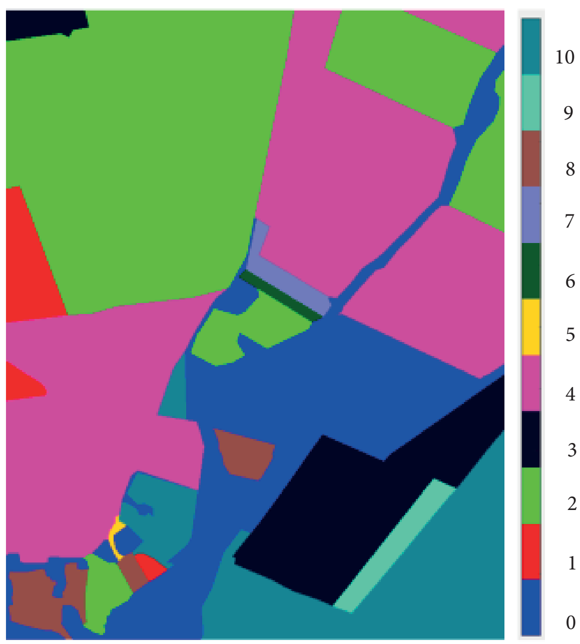

Figure 2. The ground truth.

4.2. Description of performance evaluation and implementation details

In this work, the metric used for assessing the classification performance is percentage correct [19]. It is the ratio of total number of samples classified correctly to the total number of samples classified. The software implementation is realized using the R program [20]. The package "raster" [21] is used for SAR time-series data read/write processes. The package "FNN" [22] is used in the implementation of CGLDA. The package "class" [23] is used for KNN.

4.3. Dimension reduction parameter tuning experiment

The CGLDA method requires 4 parameters to be determined and these parameters are calculated in a similar way to [13] and [14]. Parameter k is selected as in [13]. Since the features are normalized, parameter t is chosen as 1.0 [14]. For determining the other parameters ε and α, a much smaller group of pixels is selected randomly from the dataset. For each class, 500 random samples are selected to form a parameter tuning set of 5000 samples. In the tuning process, 100 samples from each class are selected to train the classifier and classification is applied on the whole tuning set. KNN is selected for the classifier with number of neighbors set to 7 and distance metric is selected as Euclidean. The tuning process is repeated 10 times and the average of the obtained overall accuracy is taken into account. Size of the high-dimensional vector space is reduced to 9. In a similar manner as in [13], ε and α parameters are tuned between 0.5 and 0.9 with step size of 0.1. Parameters yielding the highest overall classification accuracy are found to be 0.5 and 0.9 for ε and α, respectively.

4.4. Comparative performance experiment

In order to assess the performance of the proposed framework, five methods are compared with each other in terms of classification performance and computation time. These methods are D336 (using morphological operators to obtain 336-dimensional feature space without dimension reduction), the proposed method (PM, using morphological operators to obtain 336-dimensional feature space and reduction to 9 dimensions using CGLDA), PCA9 (using morphological operators to obtain 336-dimensional feature space and reduction to 9 dimensions using PCA), D16 (using time-series data of 16 features without dimension reduction and morphological operators), and the Sakarya and Demirpolat method [14] (SDM, using D16 data and reduction to 9 dimensions using CGLDA). In the experiment setup, overall classification accuracy and computation time are calculated with respect to different numbers of training samples for each class; 25, 50, 75, 100, 125, 150, 175, and 200 samples are randomly selected for each class in the experiments. The classifications are performed on the whole dataset. Performance indicators are calculated by taking the arithmetic mean of 10 repetitions of the algorithms.

The results for the overall classification performance are shown in Figure 3. The proposed method achieves the best performance for every selection of size of the training set. For the analysis of computing time performances, the approach taken in [24] is preferred. In the Table, the execution times are normalized with the minimum execution time, which is obtained with PM using 25 training samples for each class. PM, PCA9, and SDM use 9-dimensional feature space; thus, their computation times are found to be similar. According to experiments, the proposed method provided around 1% to 4% improvement in overall classification accuracy and a speed up to 529 times when compared with the D336 depending on the training set size.

Table. Comparative normalized execution-time ratio analysis according to training sample size.

Sample size	PM	D336	D16
25	1.00	86.39	1.46
50	1.56	563.15	2.31
75	2.07	869.27	3.14
100	2.64	1177.53	4.00
125	3.10	1481.44	4.84
150	3.67	1803.50	5.73
175	4.13	2135.38	6.45
200	4.63	2449.35	7.29

Figure 3 and the Table reveal that the proposed method overcomes the time complexity stemming from the morphological profile-originated high-dimensional feature space; it also improves the classification performance by using global and local pattern information.

4.5. Variable dimension size experiment

For finding the optimal dimension size, an experiment is realized. Training samples are fixed to 100 samples for each class and dimension size is increased from 3 to 50. The average of 10 randomly repeated experimental results is used in order to overcome the training sample dependence. The same classifier with the same parameters is used for classification purposes. The CGLDA and PCA methods are analyzed in the experiments. According to the experimental results demonstrated in Figure 4, the best performance of CGLDA is obtained at dimension size of 10 and the average classification performance value is 0.9116. On the other hand, the classification performance value is 0.9113 at the dimension size of 9 where the difference can be considered insignificant. Therefore, the dimension size of 9 can be an acceptable optimal dimension size for this dataset when not only the classification performance but also the time complexity is considered.

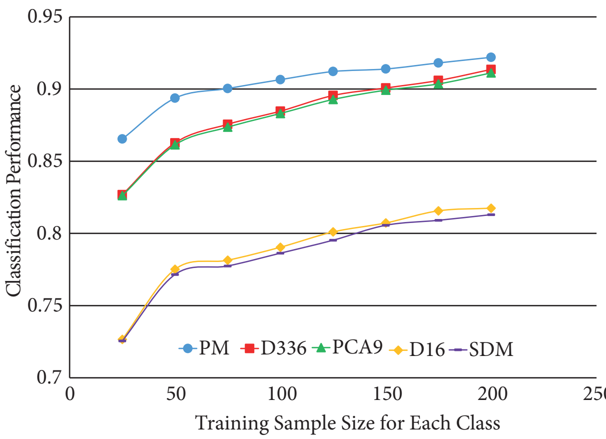

Figure 3. Comparative classification performance analysis. Training sample versus classification performance.

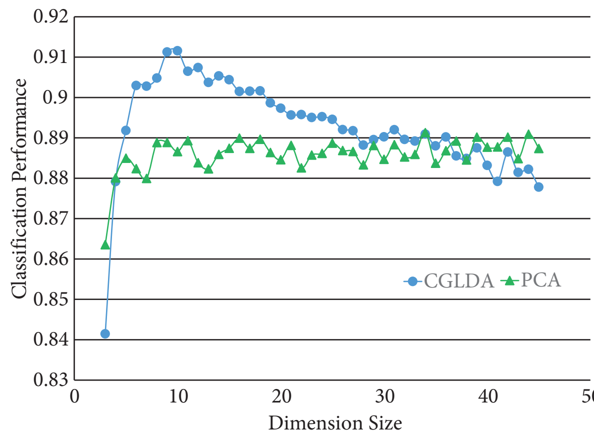

Figure 4. Comparative performance analysis. Dimension size versus performance.

4.6. Visualization of the proposed method's results

For visualization of the proposed method's results, an experiment is realized. Training samples are fixed to 100 samples for each class and dimension size is set to 9. Figure 5 demonstrates one of the results of the proposed method (accuracy = 0.8989, kappa = 0.8643) with respect to the ground truth. According to Figure 5, some postprocessing techniques may increase performances, especially for falsely classified small areas covered by correctly classified samples.

5. Conclusions

In this study, a method for crop classification that combines existing spectral and temporal information with spatial information extracted from SAR data is presented. The high-dimensional feature space is obtained by combining the original spectral and temporal information with morphological opening and closing profiles derived from time-series dual-polarized TerraSAR-X images. Global and local information-based linear discriminant analysis is used for dimension reduction of the feature space. Experimental results revealed that

Figure 5. (Left) One of the results of the proposed method (dimension = 9, training sample size for each class = 100, accuracy = 0.8989, kappa = 0.8643); (Right) Ground-truth.

the proposed method outperforms the scenarios in which no dimension reduction technique is applied in both classification and time performances. In addition, the contribution of morphological profiles to crop classification performance is significant and resulting time complexity is decreased significantly by CGLDA. It has been experimentally shown that the proposed method has significant potential to be an effective solution to supervised crop classification problems when time-series SAR data are available.

Acknowledgments

This work was conducted within the scope of the "GAP Bölgesi'nde Hassas Tarım ve Sürdürülebilir Uygulamaların Yaygınlaştırılması Projesi (HASSAS)" project funded by the Ministry of Industry and Technology of the Republic of Turkey, GAP Bölge Kalkınma İdaresi Başkanlığı. The authors are thankful to the German Aerospace Center (DLR) for providing TerraSAR-X data as a part of Project LAN3167.

References

[1] Skriver H, Mattia F, Satalino G, Balenzano A, Pauwels VRN, Verhoest NEC, Davidson M. Crop classification using short-revisit multitemporal SAR data. IEEE J Sel Top Appl Earth Obs Remote Sens 2011; 4: 423-431.

[2] McNairn H, Shang J, Champagne C, Jiao X. TerraSAR-X and RADARSAT-2 for crop classification and acreage estimation. In: Proceedings of IGARSS; 12–17 July 2009; Cape Town, Africa. pp. 898-901.

[3] Mirzaee S, Motagh M, Arefi H, Nooryazdan M. Classification of agricultural fields using time series of dual polarimetry TerraSAR-X images. Int Arch Photogramm Remote Sens Spat Inf Sci 2014; 40: 191.

[4] Blaes X, Vanhalle L, Defourny P. Efficiency of crop identification based on optical and SAR image time series. Remote Sens Environ 2005; 96: 352-365.

[5] Lardeux C, Frison PL, Tison C, Souyris JC, Stoll B, Fruneau B, Rudant JP. Support vector machine for multifrequency SAR polarimetric data classification. IEEE T Geosci Remote Sens 2009; 47: 4143-4152.

[6] Tan CP, Koay JY, Lim KS, Ewe HT, Chuah HT. Classification of multi-temporal SAR images for rice crops using combined entropy decomposition and support vector machine technique. Prog Electromagn Res 2007; 71: 19-39.

[7] Fukuda S, Hirosawa H. A wavelet-based texture feature set applied to classification of multifrequency polarimetric SAR images. IEEE T Geosci Remote Sens 1999; 37: 2282-2286.

[8] Demirkesen C, Demirpolat C, Teke M. Tarımsal alanların çok zamanlıTerraSAR-X görüntülerinde morfolojik profiller kullanılarak sınıflandırılması. In: IEEE 24. Sinyal İşleme, İletişim ve UygulamalarıKurultayı; 16–19 May 2016; Zonguldak, Turkey. pp. 1701-1704 (in Turkish).

[9] Demirpolat C, Teke M. Crop classification with morphological profiles derived from SAR and electro-optical satellite data. In: 2017 8th International Conference on Recent Advances in Space Technologies; 19–22 July 2017; İstanbul, Turkey. pp. 119-124.

[10] He C, Han G, Feng D, Du J, Liao M. A sparse manifold classification method based on a multi-dimensional descriptive primitive of polarimetric SAR image time series. ISPRS Int J Geo-Information 2017; 6: 97.

[11] Duda RO, Hart PE, Stork DG. Pattern Classification. 2nd ed. New York, NY, USA: Wiley, 2001.

[12] Zhang D, He J, Zhao Y, Luo Z, Du M. Global plus local: a complete framework for feature extraction and recognition. Pattern Recognit 2014; 47: 1433-1442.

[13] Sakarya U. Hyperspectral dimension reduction using global and local information based linear discriminant analysis. ISPRS Ann Photogramm Remote Sens Spat Inf 2014; 2: 61.

[14] Sakarya U, Demirpolat C. SAR image time series analysis in vegetation classification using global and local information based linear discriminant analysis. In: Signal Processing and Communications Applications Conference; 15–18 May 2017; Antalya, Turkey. pp. 1-4.

[15] Sakarya U. Thermal infrared hyperspectral dimension reduction experiment results for global and local information based linear discriminant analysis. In: Signal Processing and Communications Applications Conference; 16–19 May 2015; Malatya, Turkey. pp. 268-271.

[16] Dalla Mura M, Benediktsson JA, Waske B, Bruzzone L. Morphological attribute filters for the analysis of very high resolution remote sensing images. In: Proceedings of IGARSS; 12–17 July 2009; Cape Town, Africa. p. III-97.

[17] European Space Agency. Sentinel Application Platform [Online]. http://step.esa.int/main/third-party-plugins-2/sen2cor.

[18] Yu Y, Acton ST. Speckle reducing anisotropic diffusion. IEEE T Image Process 2002; 11: 1260-1270.

[19] Foody GM. Status of land cover classification accuracy assessment. Remote Sens Environ 2002; 80: 185-201.

[20] R Core Team. R: A Language and Environment for Statistical Computing. Vienna, Austria: R Foundation for Statistical Computing.

[21] Hijmans RJ. Raster: Geographic Data Analysis and Modeling. R Package Version 2.3-24 [Online]. http://CRAN.R-project.org/package=raster.

[22] Beygelzimer A, Kakadet S, Langford J, Arya S, Mount D, Li S. FNN: Fast Nearest Neighbor Search Algorithms and Applications. R package version 1.1 [Online]. http://CRAN.R-project.org/package=FNN.

[23] Venables WN, Ripley BD. Modern Applied Statistics with S-PLUS. 3rd ed. New York, NY, USA: Springer, 2013.

[24] Sakarya U, Telatar Z, Alatan AA. Dominant sets based movie scene detection. Signal Process 2012; 92: 107-119.